Mon. Not. R. Astron. Soc. **000**, 1–11 (2002) Printed 9 May 2008 (MN LaTeX style file v2.2)

arXiv:0803.1329v2 [astro-ph] 9 May 2008

Cyanopolyynes in hot cores: modelling G305.2+0.2

J. F. Chapman[1][⋆], T.J. Millar[2], M. Wardle[1] , M.G. Burton[3], A.J. Walsh[4]
[1] *Department of Physics, Macquarie University, Sydney, NSW, 2109, Australia*
[2] *Astrophysics Research Centre, School of Mathematics and Physics, Queens University Belfast, Belfast BT7 1NN, UK*
[3] *School of Physics, University of New South Wales, Sydney, NSW, 2052, Australia*
[4] *School of Maths, Physics and IT, James Cook University, NSW, 4811, Australia*

Accepted 1988 December 15. Received 1988 December 14; in original form 1988 October 11

ABSTRACT

We present results from a time dependent gas phase chemical model of a hot core based on the physical conditions of G305.2+0.2. While the cyanopolyyne HC_3N has been observed in hot cores, the longer chained species, HC_5N, HC_7N, and HC_9N have not been considered typical hot core species. We present results which show that these species can be formed under hot core conditions. We discuss the important chemical reactions in this process and, in particular, show that their abundances are linked to the parent species acetylene which is evaporated from icy grain mantles. The cyanopolyynes show promise as 'chemical clocks' which may aid future observations in determining the age of hot core sources. The abundance of the larger cyanopolyynes increase and decrease over relatively short time scales, $\sim 10^{2.5}$ years. We present results from a non-LTE statistical equilibrium excitation model as a series of density, temperature and column density dependent contour plots which show both the line intensities and several line ratios. These aid in the interpretation of spectral line data, even when there is limited line information available.

Key words: stars:formation - ISM: molecules.

1 INTRODUCTION

Hot cores are observed in regions of high mass star formation, and are small, hot ($\sim$ 200K) and dense ($\sim 10^6 \mathrm{cm}^{-3}$) clumps of gas (e.g., Sweitzer 1978; Pauls et al. 1983, for a review see, e.g., van der Tak 2003). The chemistry of these regions is unique, characterized by unusually high abundances of saturated molecules, such as H_2O and NH_3 (e.g., Henkel et al. 1987; Walmsley et al. 1987; Olmi et al. 1993). This unique chemistry is believed to be a direct result of grain mantle evaporation due to an event, such as the switching on of a nearby star or a source within the core itself (e.g., Kaufman et al. 1998; Wyrowski & Walmsley 1996). During an earlier high density phase of collapse, these molecules are formed on the surface of dust grains (e.g., Walmsley & Schilke 1991), released into the gas phase during the onset of heating, and are processed into daughter species. Since cores are both hot and dense, the time dependent gas phase chemistry rapidly changes over time scales <100,000 years. Species with time dependent chemistry can be used as 'chemical clocks' and may help in determining the age of hot core regions (e.g., Millar, Macdonald & Gibb 1997).

The origins of some interstellar molecules found in hot cores can be separated into the following three groups. Those that are formed in the cold gas:

e.g., CO, C_2H_2, C_2H_4, N_2, O_2, CS,

those formed on grain surfaces:

e.g., H_2O, CH_4, NH_3, H_2S, CH_3OH, H_2CO, C_2H_5OH, CO_2, HCOOH, NH_2CHO, C_2H_4, C_2H_6,H_2CS, OCS,

and those formed in the hot gas (e.g., Charnley 1995)

e.g., CH_3OCH_3, CH_2CO, CH_3CHO, $HCOOC_2H_5$, CH_3COCH_3, $(C_2H_5)_2O$, $CH_3OC_2H_5$, C_2H_5CN, CH_3CN, HCN, SO, SO_2, C_2H_3CN, HC_3N, CH_3NH_2, CH_2NH, SiO.

Observations of hot cores include molecular line and dust continuum emission, and some of the chemical core models, along with radiative transfer calculations, have proven useful in reproducing observed column densities (e.g., Millar, Macdonald & Gibb 1997; Kaufman et al. 1998; Thompson et al. 1999; Doty et al. 2002). Chemical models have been developed that include a pre-stellar phase or initial conditions assuming the presence of evaporated grain mantle species (e.g., Brown, Charnley & Millar 1988; Millar, Herbst & Charnley

---

[⋆] E.mail: jchapman@physics.mq.edu.au

1991; Charnley, Tielens, & Millar 1992; Caselli, Hasegawa, & Herbst 1993; Millar, Macdonald & Gibb 1997; Viti & Williams 1999; Doty et al. 2002; Nomura & Millar 2004; Wakelam et al. 2004). The injection of ice mantle material into the gas phase is usually assumed to occur instantaneously since it is driven by stellar radiation and the grain temperature rapidly increases from 10K (in the cold phase) to ∼ 200K (in the hot core) when the ices evaporate quickly. Gas-grain chemical hot core models which assume simple molecules like acetylene, C_2H_2, are released from grain mantles, have been used to account for the observed abundances of many O and N bearing molecules (e.g., Charnley, Tielens, & Millar 1992).

Carbon chain molecules make up a significant fraction of the observed interstellar molecules and cyanopolyynes HC_nN are often detected. The longer chain cyanopolyynes $HC_{2n+1}N$ (n=2-5) are associated with regions such as dark dust clouds, and are not usually associated with hot cores. $HC_{11}N$ has been detected in the interstellar medium (Bell et al. 1997), with the shorter chained species, for example HC_3N and HC_5N, more commonly associated with a number of sources including circumstellar shells and star forming regions. Cyanodiacetylene, HC_5N, is believed to be formed inefficiently in hot cores since grain mantles do not comprise of larger unsaturated molecules such as diacetylene, HCCCCH (Millar 1997). Recently, Sakai et al. (2008) detected the longer chain cyanopolyynes HC_5N, HC_7N and HC_9N towards the low-mass protostar IRAS 04368+2557 L1527. Using a gas grain model, Hassell, Herbst & Garrod (2008) modelled the chemistry of L1527, and determined that the composition of the cloud is most likely a result of warm, 30K, chemistry than cold processes.

The rotational lines from vibrational excited states of some cyanopolyynes have been detected in hot core sources. Wyrowski, Schilke & Walmsey (1999) observed a sample of six hot core sources, including G10.47+003, in vibrationally excited lines of HC_3N. Observations of the Orion Molecular cloud Core (OMC-1) have included the J = 12 → 11 transition of the $v_6 = 1$ vibrationally excited state (Goldsmith, Krotkov & Snell 1983, 1985), and 5 transitions of the $v_7 = 1$ vibrationally excited state of HC_3N. The higher cyanopolyynes are not usually detected, however, 10 rotational transitions of HC_5N and 8 transitions of HC_7N (Turner 1991) have been observed in the Orion core (OMC-1). HC_5N (Avery et al. 1979; Turner 1991) and HC_7N (Turner 1991) have also been detected in the molecular cloud of Sgr B2.

Models of the gas phase chemistry are extremely useful as predictive tools with regards to observations. However, extracting molecular abundances from line emission, suitable for comparison with the model predictions is not a straight forward task. Furthermore, although theoretical models can produce abundances for hundreds of molecules, observations are limited to specific frequency bands, and possibly contain line emission from only a handful of species. A broad understanding of the chemistry is thus not often possible with limited molecular line data for a specific source.

Modelling tools to aid in the interpretation of spectral line data are especially important for large line surveys, and efficient methods are needed to obtain physical and chemical parameters, such as column densities, relatively easily even with large numbers of species and lines. Currently, collisional rate coefficients are available for approximately 24 species on the Leiden atomic and molecular database (LAMDA) (Schoier et al. 2005), with several others in literature (e.g., CH_3CN in Green 1986), and so statistical equilibrium calculations are limited to these. Moreover, observations are limited in frequency, and so limit the process further. The list of species for which collisional rate coefficients are available include CS, OCS, SO, SO_2, SiO, HCO^+, HC_3N, HCN, HNC, H_2O, OH, CH_3OH, and NH_3. There are many more species of astronomical interest that do not appear in the LAMDA database, or elsewhere in the literature.

Table 1. The initial gas phase abundances, with respect to H nuclei, assumed in the chemical model.

Species	Abundance	Species	Abundance
CH_3OH	5×10^{-7}	C_2H_2	5×10^{-7}
NH_3	1×10^{-5}	C_2H_4	5×10^{-9}
H_2S	1×10^{-6}	C_2H_6	5×10^{-9}
H_2O	1×10^{-5}	CH_4	2×10^{-7}
O_2	1×10^{-6}	CO_2	5.0×10^{-6}
H_2CO	4×10^{-8}	OCS	5.0×10^{-8}
CO	5×10^{-5}	N_2	2×10^{-7}
He^+	2.5×10^{-11}	H^+	1×10^{-10}
H_3^+	1×10^{-8}	Si	3.6×10^{-8}
Fe^+	2.4×10^{-8}		

The aim of this paper is to model the gas phase chemistry of the hot core associated with G305.2+0.2 with particular focus on the formation of the cyanopolyynes. Non-LTE calculations are used to examine the excitation properties of these species. Section 2 outlines the chemical model with the cyanopolyyne $HC_{(3,5,7,9)}N$ chemistry discussed in Section 3. We reveal that the longer chain cyanopolyynes can be produced in appreciable abundances assuming the physical conditions of G305.2+0.2. In Section 4 we present results from a statistical equilibrium model which produces integrated line intensities. We present a series of density n_{H2}, temperature T and column density N_j dependent contour plots which will directly aid in the interpretation of observations. Non-detections of HC_5N and HC_7N from Walsh et al. (2007) in G305.2+0.2 are explained using the non-LTE model.

2 CHEMICAL MODEL

The physical model for the core is similar to that of Millar, Macdonald & Gibb (1997) and Thompson et al. (1999) which assume a spherical core geometry. The density and temperature is constant throughout since we want to examine the general gas phase chemistries. We assume a density of $n_{H2} = 8 \times 10^4 cm^{-3}$ and a temperature of 200K, which was derived for the hot core of G305.2+0.2, G305A, in Walsh et al. (2007), with a radius of 1.1pc at a distance of 3.9kpc. The current modelling work uses the latest chemical rate coefficients from Woodall, et al. (2007). The model results of Walsh et al. (2007) used the earlier Le Teuff, Millar & Markwick (2000) version. Also, the current modelling work includes the longer

Table 2. Species present in model calculations, grouped into the number n of atoms.

n = 1	H	He	N	O	C	S	Si	Fe
	H+	He+	N	O+	C+	S+	Si+	Fe
n = 2	HS	CH	NH	N2	NO	NS	CN	C2
	HS+	CH+	NH+	N2+	NO+	NS+	CN+	C2+
	CO	CS	O2	OH	SO	S2	SiS	H_2+
	CO+	CS+	O2	OH+	SO+	S2+	SiS+	
n = 3	H_2O	CH_2	NH_2	HS_2	C_2H	H_2S+	CO_2	C_2S
	H_2O+	CH_2	NH_2+	HS_2+	C_2H+	H_2S	CO_2+	C_2S+
	C_2O	SO_2	C_3	HCO	HCS	HSO+	HNS+	HSiS+
	C_2O+	SO_2+	C_3+	HCO+	HCS+	C_2N+	HN_2+	H_3+
	HCN	OCS	HNC	HSO+	HSiS+			
	HCN+	OCS+	CNC+	HNS+				
n = 4	NH_3	CH_3	C_2H_2	H_2CO	C_3H	H_2CS	C_4	C_3O+
	NH_3+	CH_3+	C_2H_2+	H_2CO+	C_3H+	H_2CS+	C_4+	C_3O
	C_3N	C_3S	H_2S_2	HOCS+	H_2NC+	HCNH+	HC_2O+	HSO_2+
	C_3N+	C_3S+	H_2S_2+	HC_2S+	H_3O+	H_3S+	HCO_2+	
n = 5	HC_3N	CH_4	C_4H	C_2H_3	C_5	C_4S	H_2CCC	C_3H_2
	HC_3N+	CH_4+	C_4H+	C_2H_3+	C_5+	C_4S+	CH_2CO+	C_3H_2+
	NH_4+	C_4N+	HCOOH	HC_3O+	H_3CS	CH_2NH	H_2CCO+	HC_3S+
	H_3CO+	H_3S_2+						
n = 6	C_5H	C_2H_4	CH_3OH	C_6	C_5N	CH_3CN	C_3H_3	H_2CCCC
	C_5H+	C_2H_4+	CH_3OH+	C_6+	C_5N+	CH_3CN+	C_3H_3+	C_3H_2O+
	CH_5+	HC_4N+	CH_2NH_2+	HC_4S+	H_2C_3H+	HC_3NH+	CH_3CO+	$HCOOH_2+$
	C_4H_2+							
n = 7	C_6H	HC_5N	CH_3CCH	C_2H_5	C_7	CH_3CHO	C_5H_2	CH_3OH_2+
	C_6H+	HC_5N+	CH_3CCH+	C_2H_5+	C_7+	CH_3CHO+	C_5H_2+	CH_3CNH+
	C_4H_3+	H_2C_4N+	CH_2CHCN	H_3C_3O+				
n = 8	C_7H	C_8	CH_3C_3N	C_6H_2	C_7N	CH_3CH_3	$HCOOCH_3$	C_3H_5+
	C_7H+	C_8+	CH_3C_3N+	C_6H_2+	C_7N+	CH_3CH_3+	$COOCH_4+$	H_2C_5N+
	C_5H_3+	C_6H_3+	CH_3CHOH+					
n = 9	C_8H	HC_7N	CH_3OCH_3	C_7H_2	C_2H_7+	CH_3C_4H	C_2H_5OH	$H_5C_2O_2+$
	C_8H+	HC_7N+	CH_3OCH_3+	C_7H_2+	C_4H_5+	CH_3C_4H+	C_2H_5OH+	CH_3C_3NH+
	C_9							
n $\geqslant$ 10	C_9H	C_9N	CH_3COCH_3	C_8H_2	HC_9N	C_9H_2	CH_3C_7N	$C_2H_5OH_2+$
	C_9H+	C_9N+	CH_3COCH_3+	C_8H_2+	HC_9N+	C_9H_2+	CH_3OCH_4+	H_2C_7N+
	C_5H_5+	C_7H_3+	CH_3COCH_4+	C_9H_3+	C_8H_3+	H_2C_9N+		
Conserved species:	e^-	H_2						

chain cyanopolyynes, HC_7N and HC_9N, along with associated species needed for their formation. These species were not considered previously in Walsh et al. (2007).

The initial gas phase abundances are given in Table 1 (e.g., Millar, Macdonald & Gibb 1997; Walsh et al. 2007). The initial abundances are based on previous models of hot cores (e.g., Millar, Macdonald & Gibb 1997, Rodgers & Charnley 2001,Walsh et al. 2007) and the mean interstellar values. The source is assumed to fill the beam, and so beam dilution does not play a large role in the model results. The model contains 245 species, consisting of the 8 elements H, He, C, N, O, Si, S, and Fe. The reaction rate network contains 3184 reactions. Included in the model are the cyanopolyynes $HC_{2n+1}N$ (n=0-4), the carbon chained molecules C_nH_2 (n=3-9) and the hydrocarbon chains C_nH (n=1-9). The full set of species are given in Table 2 with the initial mantle abundances in Table 1. The species list includes many previously observed hot core species along with essential species needed for their production.

Discrepancies between models of dense interstellar clouds (Millar, Leung & Herbst 1987) highlight the sensitivity of astrochemical models to the reaction rate coefficients as well as the reaction network. The reaction rates are taken from the most recent UMIST database which includes the latest laboratory data (Woodall, et al. 2007). The reaction networks of some of the key core species will be discussed in more detail below. Many of the rate coefficients are temperature dependent. There are a select few reactions with rate coefficients that are ill-defined outside their prescribed temperature range, with rate coefficients exponentially increasing with decreasing temperature. In these cases the rate coefficients are kept constant at the lowest or highest temperature range value nearest the temperature of interest.

Numerically, the core is described by a series of 22 concentric shells, with a density and temperature assigned to each. At each depth point or shell, the initial abundances are set and the reaction network is calculated over 10^8 years. However, the chemistry rapidly evolves over much shorter time scales than this. The species abundances are integrated along the line of sight and the column density of a species j at time t is

$$N_j(r, \theta, t) = \int_0^\infty n_j(s, t) ds \tag{1}$$

where $n_j(s, t)$ is the species abundance and s is the depth through the core along the line of sight. The coordinates r and θ specify the position of the pencil beam with respect to the centre of the core. We approximate the telescope beam using a Gaussian with an area normalized primary beam:

$$P(r) = \frac{1}{2\pi\sigma^2} \exp{(-\frac{r^2}{2\sigma^2})}, \quad \sigma = \frac{\mathrm{HPBW}}{2\sqrt{2\mathrm{In}2}} \tag{2}$$

where r is the radius measured from the centre of the gaussian and HPBW is the half power beam width. $P(r)$ is normalized so that

$$\int_0^{2\pi} \int_0^\infty P(r) r dr d\theta = 1. \tag{3}$$

To evaluate the gaussian beam, column densities are firstly evaluated along pencil beams on grid points through the chemical core model. These column densities are then convolved with the Gaussian, equation (2), giving the beam-averaged or beam diluted column density $N_j(t)$

$$N_j(t) = \frac{1}{2\pi\sigma^2} \int_0^{2\pi} \int_0^\infty N_j(r, \theta, t) \exp\left(-\frac{r^2}{2\sigma^2}\right) r dr d\theta. \tag{4}$$

3 CYANOPOLYYNES

In a related project, we have begun a survey for HC_5N in methanol-maser selected hot molecular cores from the Purcell et al. 2006 list, using the Tidbinbilla 34m telescope to measure the 31.95 GHz J=12-11 line. These results will be reported separately, when the survey is complete. However, we can report that HC_5N is frequently observed in the cores selected from this list, typically when CH_3CN 5-4 92 GHz line emission was also detected by Purcell et al. 2006. Sources have been found to contain both CH_3CN and HC_5N, or neither at all, suggesting their possible use as chemical clocks. We will explore the chemical pathways below and we show that HC_5N may well be a hot core species. We also discuss the likely role of other carbon bearing molecules.

Fukuzawa, Osamura & Schaefer (1998) have demonstrated the importance of these neutral-neutral reactions:

$$C_{2n}H_2 + CN \rightarrow HC_{2n+1}N + H, \tag{5}$$

in the formation of cyanopolyynes in the ISM. Cyanoacetylene, HC_3N is often detected in cold gas in molecular clouds, and is formed efficiently via the reaction:

$$C_2H_2 + CN \rightarrow HC_3N + H, \tag{6}$$

with a rate coefficient from Smith et al. 2004. Observed abundances of C_2H_2, (as well as CH_3CN and H_2CO) cannot be produced in the hot core gas phase alone, but can be accounted for in the cold phase chemistry where they are frozen out onto the grains before being released into the gas phase (e.g., Brown, Charnley & Millar 1988; Charnley & Tielens 1992; Charnley, Tielens, & Millar 1992). Lahuis & van Dishoeck (2000) found high abundances of hot C_2H_2 towards massive YSOs with ISO and concluded that the most likely origin is the evaporation of grain mantles. Maps of C_2H_2 emission at 13.7 microns with Spitzer toward Cepheus A East in Sonnentrucker et al. (2007) show that the distribution is likely due to the sputtering of acetylene in icy grain mantles. Although C_2H_2 has yet to be directly detected in interstellar ices, the upper limit is high, 10^{-5} with respect to hydrogen (Boulin et al. 1998), and the fractional abundance of C_2H_2 in Table 1 is chosen to be below this limit. Rodgers & Charnley (2001) have also demonstrated with a gas grain model that high abundances of C_2H_2 may be produced in the gas phase provided that a large enough abundance of methane is ejected from the grain mantles. Inside hot cores, C_2H_2 is released from the grain mantles and reaction (6) proceeds relatively easy for hot core temperatures (100-300K).

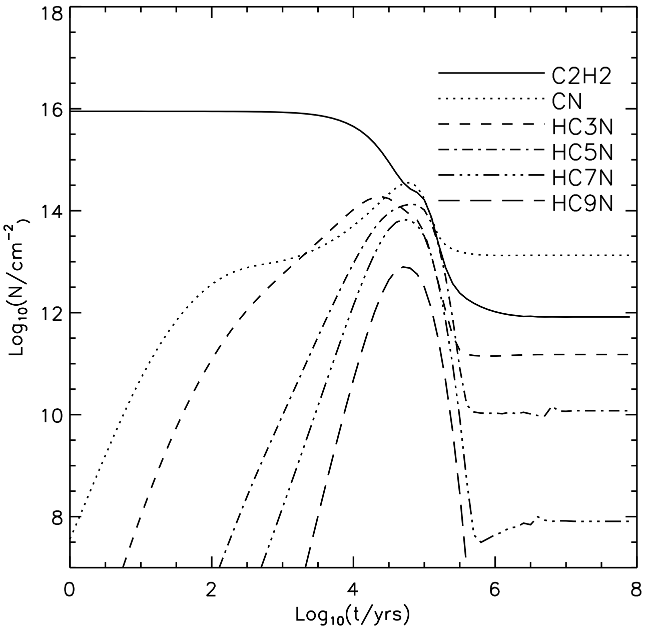

Figure 1. Time dependent column densities for the chemical model of Section 3 with $n_{H2} = 8 \times 10^4 cm^{-3}$ and a temperature of 200K. The different length cyanopolyynes are compared, along with the parent species CN and C_2H_2.

Results from the time dependent gas phase chemical model described in Section 2 are shown in Figure 1. The column density of HC_3N rises to a peak above $N=10^{14.5}cm^{-2}$ at $t=10^{4.3}$ years, and reaches its steady state abundance after 10^6 years. The abundance of HC_3N initially increases with CN since it is mainly produced via the reaction of CN with C_2H_2, reaction (6). Also plotted are the larger cyanopolyynes $HC_{5,7,9}N$, whose abundances also peak near $t=10^{4.3}$ years. These species are not usually considered hot core species but in Figure 1 they are all reach appreciable column densities over $N = 10^{12.5}$ cm^{-2}. The peak column densities of the shorter molecules, HC_5N and HC_7N, are one order of magnitude larger than that of HC_9N. Also, all species reach steady state abundances after 10^6 years.

In the ISM cyanodiacetylene, HC_5N is mainly formed in the neutral-neutral reaction

$$\mathrm{CN + H_2CCCC \rightarrow HC_5N + H}. \tag{7}$$

The rate coefficient for this reaction is 2.55×10^{-10} cm^3 s^{-1} at a temperature of 300 K (Woodall, et al. 2007). This was confirmed as the dominant reaction in the production of HC_5N in the hot core results of Figure 1. This reaction has not been considered important in the past since it was not thought that H_2CCCC was formed on the grain surfaces or very efficiently in the gas phase. However, H_2CCCC is formed efficiently via

$$\mathrm{C_2H + C_2H_2 \rightarrow H_2CCCC + H} \tag{8}$$

with a rate coefficient of 1.5×10^{-10} cm^3 s^{-1} at 200K. The column densities of H_2CCCC and C_2H are plotted in Figure 3, reaching peak column densities of $10^{14.8}$cm^{-2} and $10^{14.5}$cm^{-2}, respectively, near 10^4 years. Therefore, the abundance of H_2CCCC, and thus HC_5N, also depend on acetylene C_2H_2. CN is produced in relatively large quantities, furthering the efficiency of reaction (7). CN is produced mainly by dissociative recombination of H_2NC^+,

$$\mathrm{H_2NC^+ + e^- \quad \rightarrow \quad CN + H_2}, \tag{9}$$

and at later times after 10^5 years by the reaction

$$\mathrm{C + NO \quad \rightarrow \quad CN + O}. \tag{10}$$

H_2NC^+ is formed by

$$\mathrm{He^+ + CO \quad \rightarrow \quad O + C^+ + He} \tag{11}$$

$$\mathrm{C^+ + NH_3 \quad \rightarrow \quad H_2NC^+ + H}, \tag{12}$$

and reaction (10) is preceded by

$$\mathrm{N + OH \quad \rightarrow \quad NO + H} \tag{13}$$

$$\mathrm{H_3O^+ + e^- \quad \rightarrow \quad OH + H + H}. \tag{14}$$

Carbon chained polar molecules of the form $H_2C{=}C..C$ have been detected in the laboratory and have been identified as useful species to radio astronomers being stable under interstellar conditions. Killian et al. (1990) have detected propadienlylidene H_2CCC and butatrienylidene H_2CCCC in the laboratory, and suggest that the H_2C_n cumulene carbenes may be an another important sequence of interstellar molecules, comparable with the cyanopolyynes (HC_nN observed in space up to $n = 11$) and the linear hydrocarbon chains C_nH (observed up to n=8). H_2CCCC is an isomer of diacetylene HCCCCH and has been detected in the dark cloud TMC-1 (Kawaguchi et al. 1991) and the circumstellar shell of IRC +10216 (Cernicharo et al. 1991).

The increase of the abundance of HC_7N in Figure 1 is due to the reaction network

$$\mathrm{C_2H_2 + C_4H \quad \rightarrow \quad C_6H_2 + H} \tag{15}$$

$$\mathrm{CN + C_6H_2 \quad \rightarrow \quad HC_7N + H}. \tag{16}$$

Once again the abundance of the cyanopolyyne HC_7N is directly related to acetylene. Similarly, the increase in the abundance of HC_9N can be accounted for by the reactions

$$\mathrm{C_6H_2 + C_2H \quad \rightarrow \quad C_8H_2 + H} \tag{17}$$

$$\mathrm{CN + C_8H_2 \quad \rightarrow \quad HC_9N + H}, \tag{18}$$

and this can be related to the HC_7N reaction network (reaction 15) via the C_6H_2 molecule. The column densities of the molecules responsible for the production of the cyanopolyynes are plotted in Figure 3 and are compared with the daughter species HC_5N, HC_7N and HC_9N in Figure 2. The abundance of H_2CCCC increases to a peak of $10^{14.8}$cm^{-2} at 10^4 years. The abundance of the daughter species HC_5N also increases reaching a peak of $10^{14.2}$cm^{-2} near 10^5 years. The peak in HC_5N occurs at a later time then its parent H_2CCCC. Similar relationships between C_6H_2 and HC_7N, and between C_8H_2 and HC_9N, can also be seen.

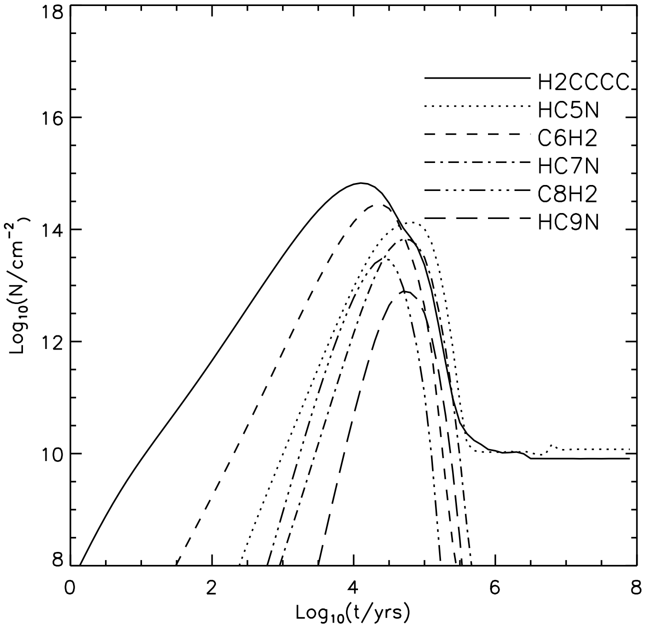

Figure 2. As for Figure 1, but for a comparison of the higher order cyanopolyynes HC_nN (n>3) with their parent species.

The formation of the cyanopolyynes, HC_5N , HC_7N and HC_9N, are sensitive to the abundances of CN and the carbon chain molecules H_2CCCC, C_6H_2, and C_8H_2. Furthermore, the abundance of the carbon chain molecules are dependent on acetylene C_2H_2. Thus one would expect, that if C_2H_2 is present in the gas then the larger cyanopolyynes may also be present. Figure 4 illustrates this, showing the resulting abundances when no C_2H_2 is initially evaporated from grain mantles. The acetylene abundance initially increases to a column density $\sim 10^{14}$cm^{-2} near $10^{4.3}$ years. HC_3N, HC_5N, HC_7N and HC_9N reach peak densities of $10^{13.5}$cm^{-2}, $10^{12.7}$cm^{-2}, $10^{11.8}$cm^{-2}, and $10^{10.4}$cm^{-2}, respectively. These column densities are a magnitude (or in some cases less) smaller then those of Figure 1.

Since CH_3CN emission is often used as a signature of the presence of a hot molecular core, we have investigated its relative abundance compared to HC_5N as a function of time. CH_3CN is efficiently produced via

$$\mathrm{CH_3CNH^+ + e^- \quad \rightarrow \quad CH_3CN + H} \tag{19}$$

and the abundance of CH_3CNH^+ is driven by radiative association:

$$\mathrm{CH_3^+ + HCN \rightarrow CH_3CNH^+ + } h\nu. \tag{20}$$

The methyl cyanide chemistry is shown in Figure 5. For the first 10^4 years, CH_3^+ is produced by

$$\mathrm{H_3{}^+ + CH_3OH \quad \rightarrow \quad CH_3^+ + H_2O + H_2} \tag{21}$$

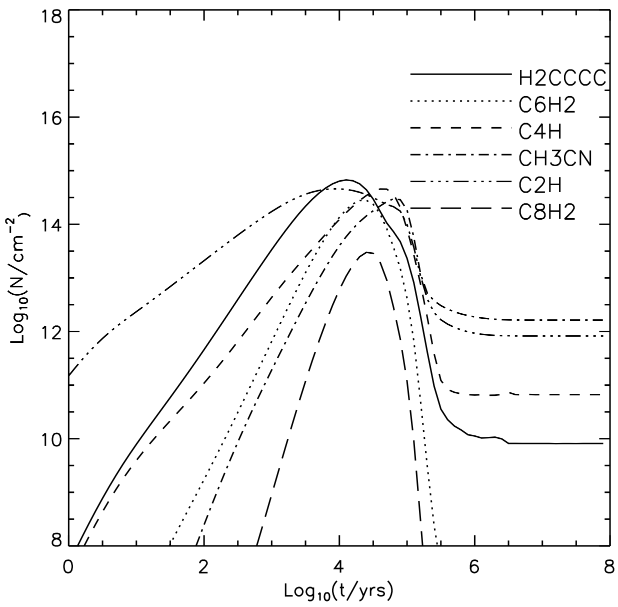

Figure 3. As for Figure 1, but for the parent species of the higher order cyanopolyynes HC_nN (n>3).

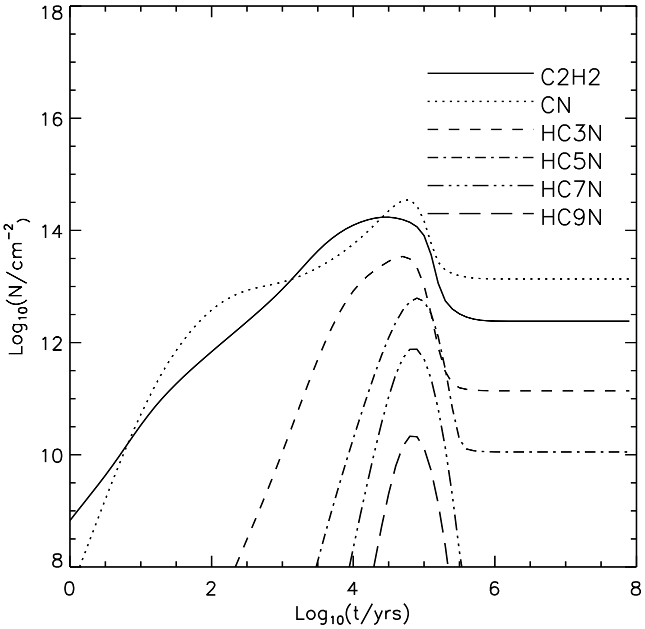

Figure 4. As for Figure 1, however, C_2H_2 is assumed to form in the gas only, with no initial abundance related to grain mantle evaporation.

and

$$H_2 + CH_2^+ \quad \rightarrow \quad CH_3^+ + H \tag{22}$$

thereafter. The HCN abundance is driven by

$$NH_3 + HCNH^+ \quad \rightarrow \quad HCN + NH_4^+ \tag{23}$$

for the first 10^5 years and

$$HCNH^+ + e^- \quad \rightarrow \quad HCN + H \tag{24}$$

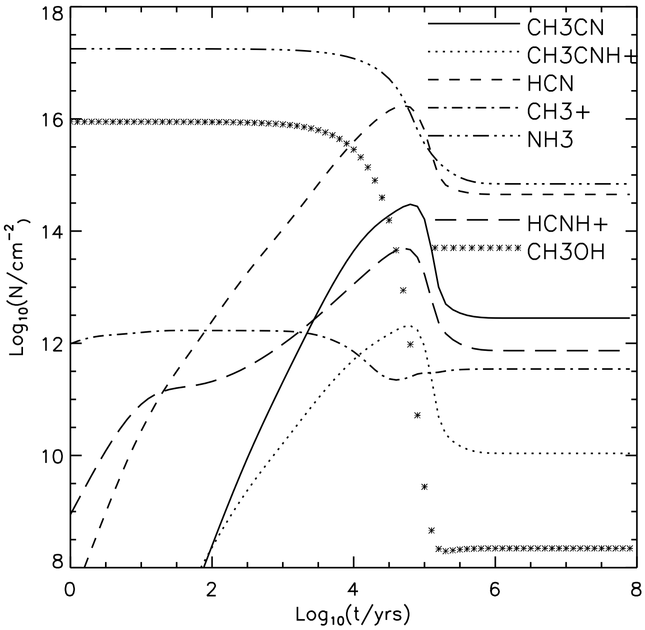

Figure 5. As for Figure 1, but shows the parent species responsible for the formation of CH_3CN.

after 10^5 years. These are preceded by

$$H_2 + HCN^+ \quad \rightarrow \quad HCNH^+ + H \tag{25}$$

$$C^+ + NH_3 \quad \rightarrow \quad HCN^+ + H_2 \tag{26}$$

$$C^+ + NH_2 \quad \rightarrow \quad HCN^+ + H. \tag{27}$$

In Figure 5, the destruction of the mantle species NH_3 and CH_3OH begins near 10^4 years, signalling the start of the rapid gas phase chemistry between 10^4 and 10^5 years. As reaction (23) proceeds, the HCN abundance increases. CH_3^+ is strongly dependent on CH_3OH which is highly abundant before 10^4 years and so remains in the gas phase with a constant column density of $10^{12}cm^{-2}$ between 10^2 and 10^4 years. When the abundance of HCN increases, reaction (20) proceeds and the abundance of CH_3CNH^+ increases, allowing the formation of CH_3CN via reaction (19).

The abundances of HC_5N and CH_3CN are not directly linked via their respective reaction networks, however the abundances of both are strongly dependent on their parent grain mantle species. The abundances of both increase at the onset of the rapid gas phase chemistry caused by the destruction of the grain mantle species. As a useful comparison, we plot the time dependent HC_5N/CH_3CN ratio in Figure 6. The ratio increases considerably between 10^4 and $10^{5.5}$ years and so could prove useful in determining the age of hot cores within this range.

4 MOLECULAR LINE EXCITATION MODEL

In this section, a molecular excitation model is used to calculate the excitation of HC_3N, HC_5N and HC_7N. The collisional rates (per second per molecule) with H_2 are taken from the LAMDA database (Schoier et al. 2005). Only collision rates for the ground vibrational state are currently available in the database and it outside the scope of this work to consider the higher vibrational transitions. We note

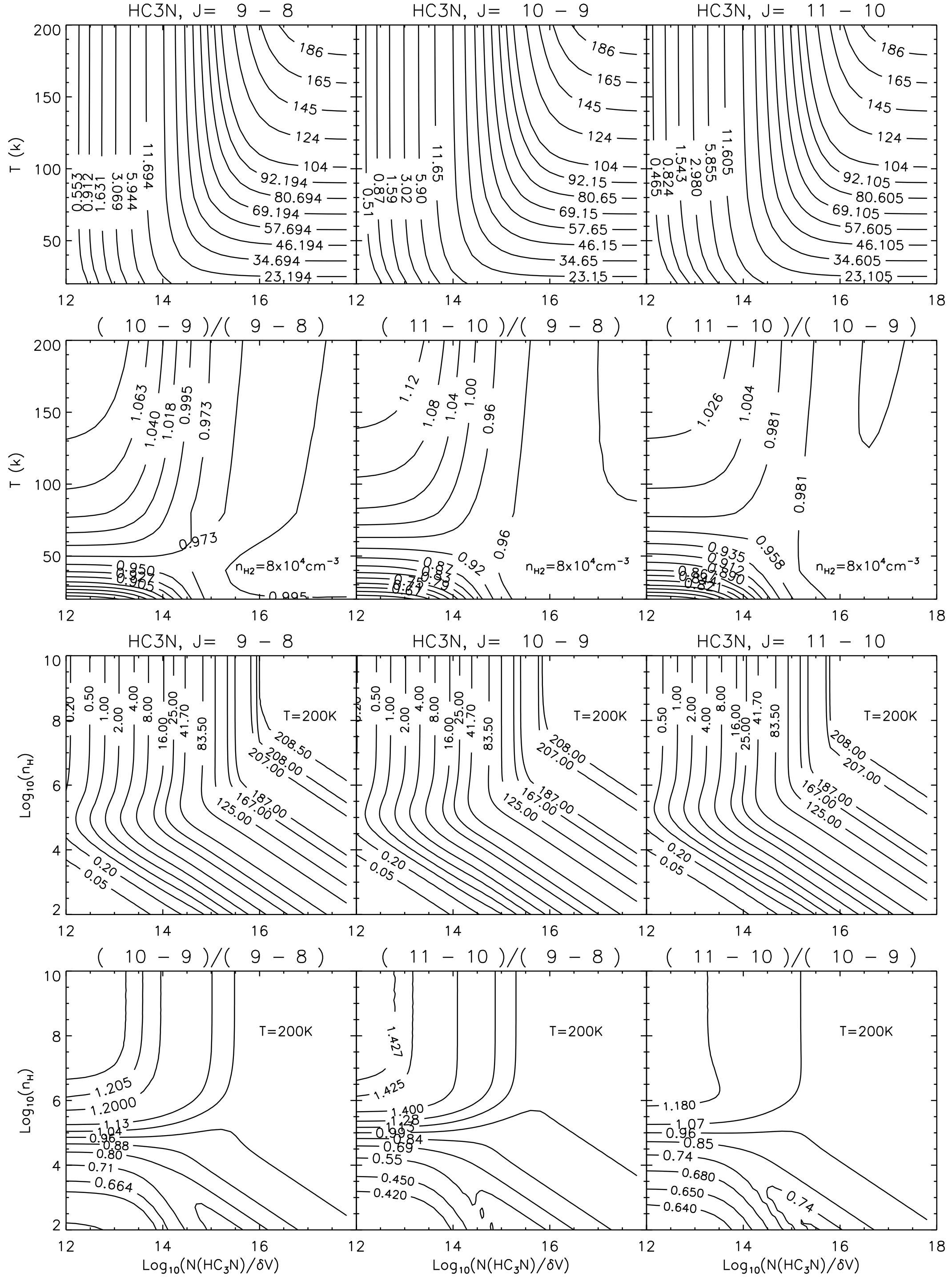

Figure 7. Line intensities and ratios of HC_3N for the J=9-8 (81.88GHz), J=10-9 (90.98GHz) and J=11-10 (100.08GHz) lines calculated by the excitation model. The first row shows the line intensities in units of K km/s as a function of temperature and column density (normalised by line width) assuming a density of $n_{H2} = 8 \times 10^4 cm^{-3}$. In the second row, three line ratios as a function of temperature and column density for constant density $8 \times 10^4 cm^{-3}$ are plotted. In the third and fourth rows, the corresponding plots as a function of density for a constant temperature of 200K are shown.

however, that although higher vibrational lines of HC_3N have been observed in SgB2 (Goldsmith, Krotkov & Snell 1983, 1985), Walsh et al. (2007) did not detect any higher vibrational transitions of HC_3N, HC_5N or HC_7N in G305A. Here we only consider the ground vibrational states and will have to wait until the collision rates are available for higher states to update our model in the future.

The collision rates depend on the cross section of HC_3N and the density of H_2. The LAMDA database also contains the relevant transitional frequencies, rotational levels and

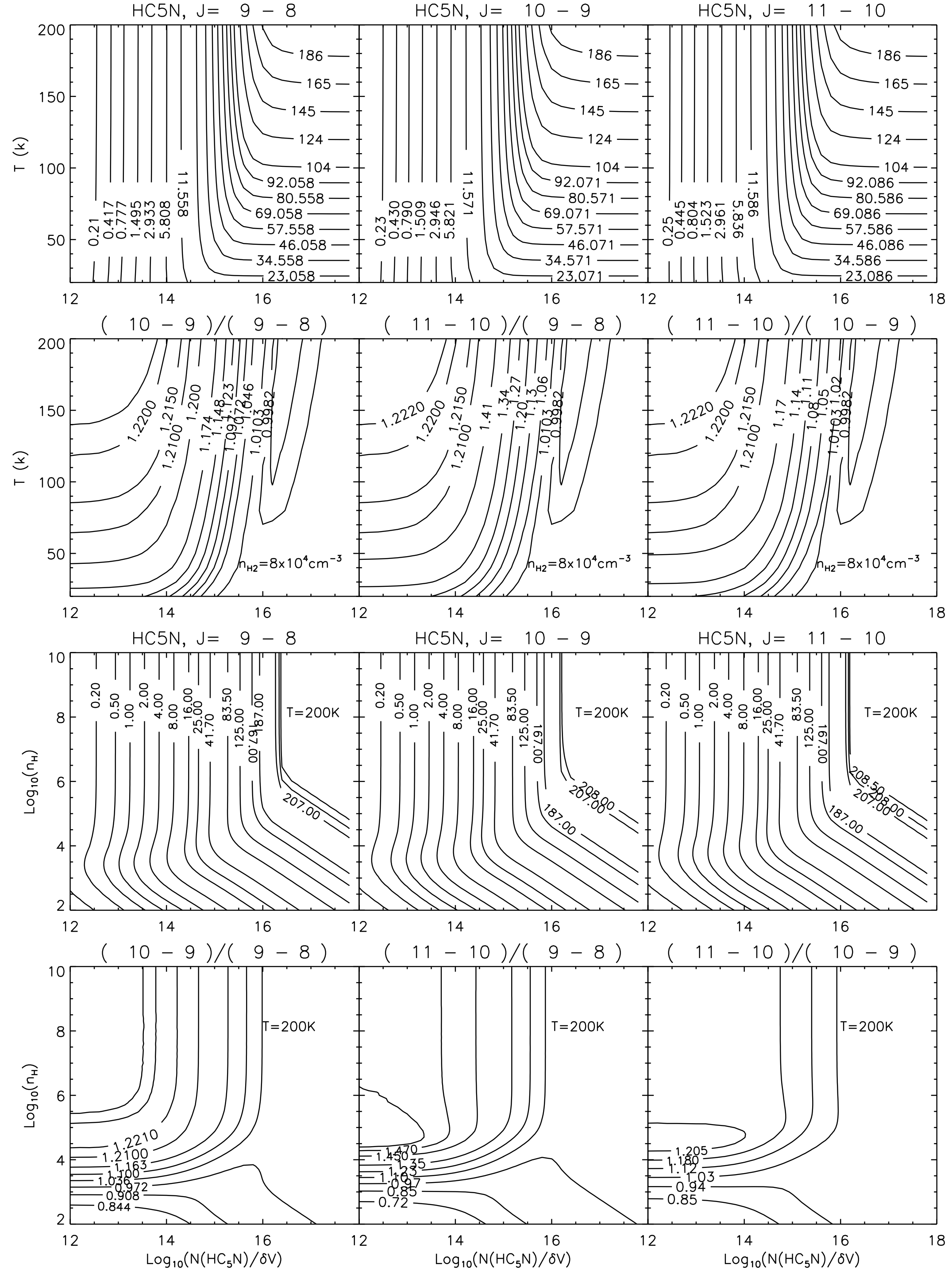

Figure 8. As for Figure 7 but for the J=9-8 (23.96GHz), J=10-9 (26.63GHz) and J=11-10 (29.29GHz) lines of HC_5N.

Einstein A-coefficients for 24 molecules compiled from sources such as the JPL Molecular Spectroscopy database (Pickett et al. 1998) and the CDMS catalogue (Muller et al. 2005). The escape probability method is used here to simplify the statistical equilibrium equations (see for example Schoier et al. 2005), with the model outputting the intensity of a line for a given density and temperature. Similar model calculations for other species of interest can be found in, for example, Liszt (2006), Lique, Cernicharo & Cox (2006), Daniel, Cernicharo & Dubernet (2006), van der Tak & Hogerheijde (2007), and Walsh et al. (2007).

In Figure 7, line intensities and line ratios are plotted for the 81.88, 90.98 and 100.08GHz rotational lines of HC_3N. The LAMDA database (Schoier et al. 2005) contains collision rates of the first 21 levels (9-181GHz) of HC_3N (however the higher transitions are affected by truncation). These plots are useful in interpreting observations since a measured

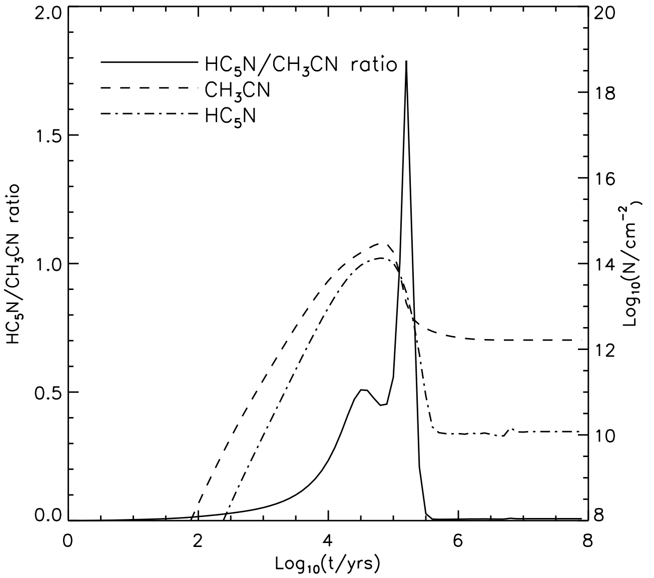

Figure 6. Time dependent HC_5N/CH_3CN ratio for model in Figure 1.

line intensity, or line ratio can directly be compared on the plot, and the column density and/or density may be determined. In the first row, the individual line intensities in units K kms^{-1} are given for a density of $n_{H2} = 8 \times 10^4 cm^{-3}$ as a function of temperature and column density. Each plot shows the same overall trends, with the intensities becoming relatively constant with temperature for given normalised column densities below $10^{14}cm^{-2}$. A single observed line intensity could be directly compared to these, after telescope beam dilution effects have been taken into account. As illustrated in, for example, (Walsh et al. 2007), plotting multiple lines from non-LTE models allows for the determination of the column density, as well as putting limits on the density and temperature of the region.

We also show in the second row of Figure 7 the line ratios as a function of temperature for $n_{H2} = 8 \times 10^4 cm^{-3}$, which do not require any correction for beam dilution effects. The intensity of the 100.08GHz (J=11-10) line is strongest (for a given temperature and density), then the 90.98GHz (J=10-9) and 81.88GHz (J=9-8) lines. In the hot core regime, for temperatures of the order 150K and above, the ratios are relatively constant with column density and so potentially allowing one to read off the column density directly using an observed line ratio value.

In the third row of Figure 7, the line intensities are shown again, but this time as a function of density for T=200K. Each contour becomes constant with column density as the density increases, and the LTE approximation is approached with increasing n_{H2}. One could safely assume the LTE approximation, and use a rotation diagram, for densities above $10^6 cm^{-3}$ and if the line width normalised HC_3N column density is expected to be in the range $10^{12}cm^{-2}$ to $10^{16}cm^{-2}$. Finally, in the bottom row of Figure 7, the line ratios are plotted as a function of density. As the column density decreases, the contours become constant with density. The trend towards LTE with increasing density is also clear.

Depending on what information is available, either series (row) of plots in Figure 7 may be the most useful in interpreting observations. If either the temperature or density is known than the complexity is reduced greatly, and the corresponding plots with the appropriate temperature or density can be produced. Notwithstanding, however, even if these are unknown, the combination of all four plots can still be useful in determining limits on the density, temperature and column density. Collision rates for the larger cyanopolyynes HC_5N, HC_7N, HC_9N etc. have yet to be published. To calculate the excitation of HC_5N, we have used the collisional rates of HC_3N (Schoier et al. 2005), however the cross section for HC_5N is scaled by a factor of 1.5 to account for the greater geometric length (e.g., Avery et al. 1979; Snell et al. 1981). The energy levels and Einstein A coefficients for HC_5N have been taken from the CDMS database (Muller et al. 2005). The collision rates for HC_3N are available for the first 21 lines and in the case of HC_5N this includes all transitions from 2GHz to 54GHz. In Figure 8 the corresponding line intensities and line ratios are plotted for the 23.96, 26.63 and 29.29GHz lines of HC_5N, showing similar characteristics as for HC_3N. A similar calculation has also been performed for HC_7N, after scaling the collision rates of HC_3N by 2 to account for the larger cross section of HC_7N (plots not shown here). These plots show similar features as those for HC_3N and HC_5N.

In the ATCA observations of Walsh et al. (2007) the HC_5N(7-6) 18.64GHz and HC_7N(15-14) 16.92GHz lines were not detected in G305A, although Figure 1 suggests that these species are likely produced in this region. We will now address this issue. The 1σ upper limits of the integrated intensity of these non-detections from the ATCA observations were <0.11Kkm/s and <0.03Kkm/s, for HC_5N(7-6) and HC_7N(15-14), respectively. Using the non-LTE model, we plot the upper limit intensities of each of these lines in Figure 9 for a temperature of 200K, and varying density. We also plot the observed HC_3N(2-1) 18.20GHz line for comparison, this line was already considered in the non-LTE analysis of Walsh et al. (2007). For a density of $n_{H2} = 8 \times 10^4 cm^{-3}$, the following limits are imposed on the normalized column densities; $N_{HC_5N}/\delta V < 3.16 \times 10^{12}$ and $N_{HC_7N}/\delta V < 3.89 \times 10^{11}$. In Walsh et al. (2007) an age range for G305A of $2 \times 10^4 < t_{core} < 1.5 \times 10^5$ year was imposed, based on all the detected lines. From Figure 1, this age range implies column densities of $10^{13}cm^{-2} < N_{HC_5N} < 10^{14}cm^{-2}$ and $2.5 \times 10^{12}cm^{-2} < N_{HC_7N} < 6.3 \times 10^{13}cm^{-2}$, with the lower limits defined by the later core age of 1.5×10^5 years. After, assuming a line width of > 3.2km/s for the lines in Figure 9, which is not unreasonable, the column densities of HC_5N and HC_7N agree with Figure 1 for a core range of the order 1.5×10^5 years. The NH_3 observations of Walsh et al. (2007) favor a later age for G305A of the order 10^5 years, also. Around this time the cyanopolyynes are being destroyed, and their column densities decrease rapidly. This could explain why these species were not detected in Walsh et al. (2007), since there abundance was not high enough to be detected.

5 DISCUSSION

The results from the chemical model in Sections 2 and 3 show that the cyanopolyynes switch on after 10^2 years and

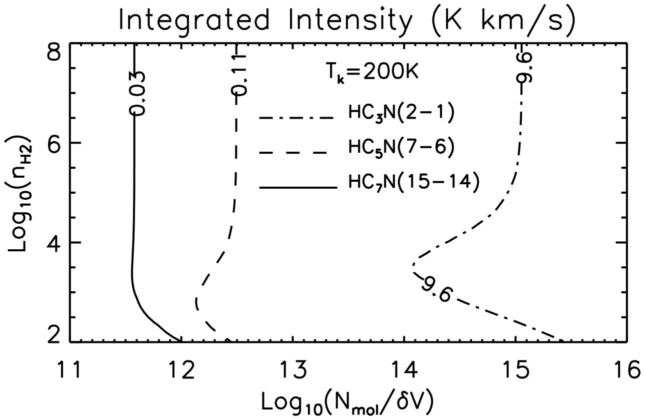

Figure 9. Comparison of cyanopolyynes from (Walsh et al. 2007) using a non-LTE excitation model.

peak around $10^{4.5}$ years, before being rapidly destroyed before $10^{5.5}$ years. Acetylene was shown to be a key species in the formation of the cumulene carbenes H_2C_n, which react with CN to form the cyanopolyynes. Since acetylene is abundant in large quantities, as it has been evaporated from grain mantles, and CN is formed easily in the gas phase, the cyanopolyynes should also be found in hot cores. The formation and subsequent destruction of the longer chain cyanopolyynes are relatively short lived, which may explain why these are not often observed in hot core sources. However, if they are observed, they may prove very useful as chemical clocks, as they could help pinpoint the age of the hot core. Their detection in sources with similar physical conditions to those of G305A in Section 2 should imply ages of the order of $10^{4.5}$ years.

The calculated time dependent chemistry in Section 2 are for specific physical conditions; $n_{H2} = 8 \times 10^4 cm^{-3}$ and T=200K. We now examine the sensitivity of the chemical model results to changes in density and temperature so that these results may be extended to hot cores with different physical conditions to G305A. Since the conditions inside the core are constant throughout, and the source fills the beam and beam dilution effects are not so important, changes in the size of the core, will only scale the column densities and not change the time dependent features. Since the reaction rates are temperature dependent, a change in temperature will effect the model results. The reaction rates for two body reactions are of the form

$$k = \alpha(T/300)^{\beta}\exp(\gamma/T) \quad cm^3s^{-1} \tag{28}$$

where α, β and γ are constants taken from the UMIST database (Woodall, et al. 2007). The reaction rates for reaction (5), are the same regardless of the length of each cyanopolyyne but vary with temperature. A reduction in temperature to 100K, increases the reaction rate by 1.6 and therefore increases the abundances. This is shown in Figure 10.

Since we have only considered the physical conditions for G305.2+0.2, we now increase the density to illustrate that longer chain cyanopolyynes should also be formed in higher density cores. In Figure 11 we consider an increase the density by a factor of 10 to $n_{H2} = 8 \times 10^5 cm^{-3}$. The species abundances are enhanced by at least a factor of 10.

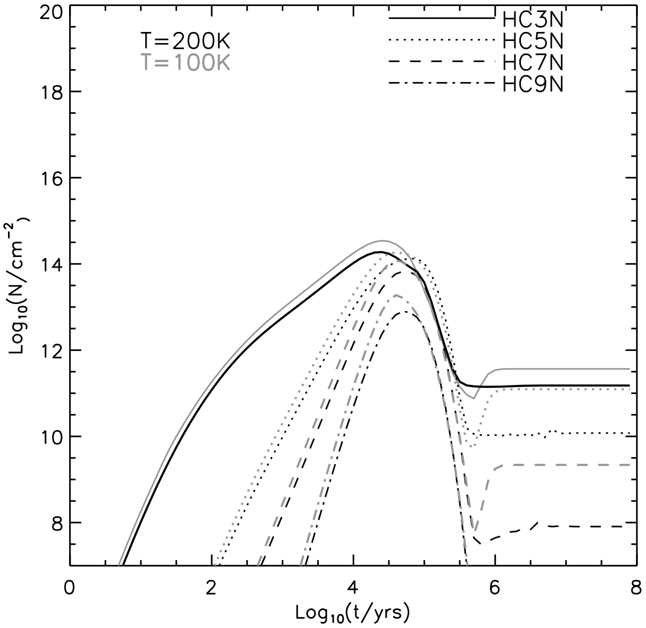

Figure 10. Comparing the time dependent chemistry for model with $n_{H2} = 8 \times 10^4 cm^{-3}$ and temperatures of 100K and 200K.

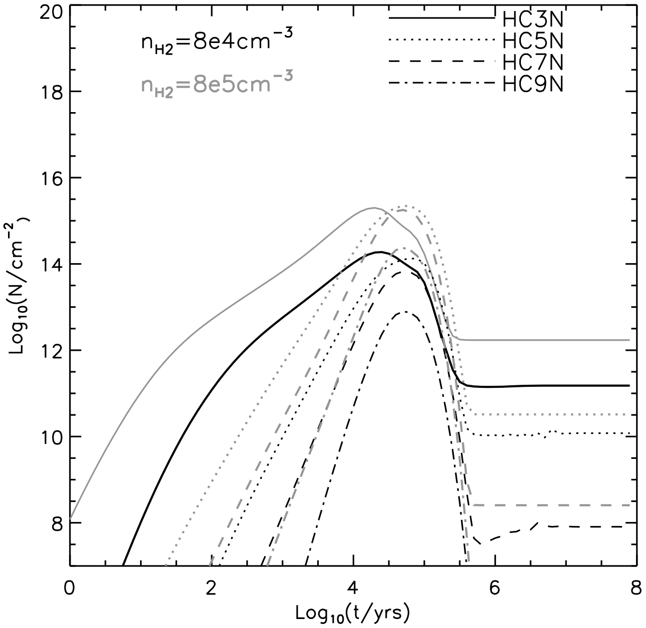

Figure 11. Comparing the time dependent chemistry for model with a temperature of 200K and densities of $n_{H2} = 8 \times 10^4 cm^{-3}$ and $n_{H2} = 8 \times 10^5 cm^{-3}$.

The time dependent features follow the same movements as for the lower density G305A case.

6 SUMMARY

In the core chemical model presented here, with density $n_{H2} = 8 \times 10^4 cm^{-3}$ and a temperature of 200K, the cyanopolyynes show highly time dependent chemistry between 10^2 and 10^6 years. Although the larger cyanopolyynes

HC_nN (n> 3) are usually not observed and have not been considered in theoretical models in the past, we have shown that they can be produced under hot core conditions. Their abundance is directly linked to acetylene, which is highly abundant in the earlier stages of the core evolution when it is evaporated from grain mantles. The reactions responsible for processing acetylene into the daughter species cyanopolyynes are efficient under the physical conditions of G305A, as well as the higher density and temperature cases considered in Section 5. The abundance of the larger cyanopolyynes increase and decrease over a short period of the order of $10^{2.5}$ years, and are relatively short lived compared with other more commonly observed species. This may explain why they have been observed in so few sources. Since they are only present in the gas phase for a relatively short time, they make useful species as chemical clocks, if the source age lies within this window. HC_3N, however, is produced in large abundances much earlier on than the larger cyanopolyynes which may explain why it has been detected in several sources.

Through the use of a molecular excitation model, we presented a series of line intensity and line ratio plots, useful for the interpretation of spectral line data of HC_3N and HC_5N. Given a series of line intensities measured from a source, these and the associated line ratios can be used to look up the column density of a species. Although there were non-detections of HC_5N and HC_7N in Walsh et al. (2007), we show that this is most probably due to these species having low column densities which are below the observing range of the ACTA.

ACKNOWLEDGMENTS

We would like to thank the anonymous referee who has helped improve the quality of this paper. This research was supported by the Australian Research Council. Astrophysics at QUB is supported by a grant from the STFC.

REFERENCES

Avery, L.W., Oka, T.,Broten, N.W., MacLeod, J.M., 1979, ApJ, 231, 48

Bell, M.B., Feldman, P.A., Travers, M.J., McCarthy, M.C., Gottlieb, C.A., Thaddeus, P., 1997, ApJ, 483, L61

Boudin, N., Schutte, W.A., Greenberg, J.M., 1998, A&A, 331, 749

Brown, P.D., Charnley, S.B., Millar, T.J., 1988, MNRAS, 231, 409

Caselli P., Hasegawa T.I., Herbst E., 1993, ApJ, 408, 548

Cernicharo, J., Gottlieb, C.A., Guelin, M., Killian, T.C., Thaddeus, P., Vrtilek, J.M., 1991, ApJL, 368, L43

Charnley, S.B., 1995, Ap&SS, 224, 251C

Charnley, S.B., Tielens, A.G.G.M., Astrochemistry of Cosmic Phenomena, IAU Symposium, Ed. Singh P.D., 1992, 150, 317

Charnley, S.B., Tielens, A.G.G.M., Millar, T.J., 1992, ApJ, 399, L71

Daniel, F., Cernicharno, J., Dubernet M.L., 2006, ApJ, 648, 471

Doty S.D., van Dishoeck E.F., van der Tak F.F.S, Boonman A.M.S., 2002, A&A, 389, 446

Fukuawa K., Osamura, Y., Schaefer H.F., 1998, ApJ, 505, 278

Goldsmith, P.F., Krotkov, R., Snell, R.L., 1983, ApJ, 274, 184

Goldsmith, P.F., Krotkov, R., Snell, R.L., 1985, ApJ, 299, 405

Green, S., ApJ, 1986, 309, 331

Hassel, G.E., Herbst E., Garrod, R.T., 2008, ApJ, In press

Henkel C., Mauersberger R., Wilson T.L., Snyder L.E., Menten K.M., Wouterloot J.G.A., 1987, A&A, 182, 299

Kaufman M.J., Hollenbach D.J., Tielens A.G.G.M., 1998, ApJ, 497, 276

Kawaguchi, K., Kaifu, N., Ohishi, M., Ishikawa, S.-I., Hirahara, Y. Yamamoto, S., Saito, S., Takano, S., Murakami, A., Vrtilek, J.M., Gottlieb, C.A., Thaddeus, P., Irvine, W.M., 1991, PASJ, 43, 607

Killian, T.C., Vrtilek, J.M., Gottlieb, C.A., Gottlieb, E.W. Thaddeus, P., 1990, ApJL, 365, L89

Lahuis, F., van Dishoeck, E.F., 2000, A&A, 355, 699

Lique, F., Cernicharo J., Cox, P., 2006, ApJ, 653, 1342

Liszt, H.S., 2006, A&A 458, 507

Millar, T.J., 1997, Models of Hot Molecular Cores, in Molecules in Astrophysics: Probes and Processes (IAU Symposium 178), ed. E F van Dishoeck, Kluwer: Dordrecht, pp. 75-88

Millar T.J., Herbst E., Charnley S.B., 1991, ApJ, 369, 147

Millar, T.J., Leung, C.M., Herbst, E., 1987, A&A, 183, 109

Millar T.J., Macdonald G.H., Gibb A.G., 1997, A&A, 325, 1163

Muller, H.S.P, Schlder, F., Stutzki, J., Winnewisser, G., 2005, J. Mol. Struct., 742, 215

Nomura H., Millar T.J., 2004, A&A, 414, 409

Olmi L., Cesaroni R., Walmsley C.M., 1993, A&A, 276, 489

Pauls A., Wilson T.L., Bieging J.H., Martin R.N., 1983, A&A, 124, 23

Pickett, H.M., Poynter, R.L., Cohen, E.A., Delitsky, M.L., Pearson J.C., Muller, H.S.P., 1998, J. Quant. Spectrosc. & Rad. Transfer, 60, 883

Purcell C. R., Balasubramanyam R., Burton M. G., Walsh A. J., Minier V., Hunt-Cunningham M. R., Kedziora-Chudczer L. L., Longmore S. N., and 26 other authors, 2006, MNRAS, 367, 553

Rodgers, S.D., Charnley, S.B., ApJ, 2001, 546, 324

Sakai, N., Sakai, T., Hirota, T., Yamamoto, S., ApJ, 2008, 672, 371

Smith, I.W.M., Herbst, E., Chang, Q., 2004, MNRAS, 350, 323

Sweitzer J.S., 1978, ApJ, 225, 116

Schoier F.L., van der Tak F.F.S., van Dishoeck E.F., Black J.H. 2005, A&A, 432, 369

Snell, R.L., Schloerb, F.P., Young, J.S., Hjalmarson, A., Friberg, P., 1981, ApJ, 244, 45

Sonnentrucker, P., González-Alfonso, E., Neufeld, D.A., 2007, ApJ, 671, L37

Le Teuff, Y.H., Millar, T.J., Markwick, A.J., 2000, A&A Suppl. Ser., 146, 157

Thompson, M.A., Macdonald, G.H., Millar, T.J., 1999, A&A, 342, 809

Turner, B., 1991, ApJS, 76, 617

van der Tak F.F.S., 2003, in Star formation at high angular resolution, IAU Symp., 221, 59

van der Tak, F., Hogerheijde, M., 2007, Molecular data and radiative transfer tools for ALMA, astro-ph/0702385

Viti S., Williams D.A., 1999, MNRAS, 305, 755

Wakelam, V., Caselli, P., Ceccarelli, C., Herbst, E., Castets, A., 2004, A&A, 422, 159

Walmsley, C.M., Hermsen, W., Henkel, C., Mauersberger, R., Wilson T.L., 1987, A&A, 172, 311

Wyrowski, F., Walmsley, C.M., 1996, A&A, 314, 265

Walsh, A.J., Chapman, J.F., Burton, M.G., Wardle, M., Millar T.J., MNRAS, 2007, 380, 1703

Woodall, J, Agundez, M , Markwick-Kemper, A.J., Millar, T.J., 2007, A&A, 466, 1197

Wyrowski, F., Walmsley, C.M., 1996, A&A, 314, 265

Wyrowski, F., Schilke, P., Walmsey, C. M., 1999, A&A, 341, 882